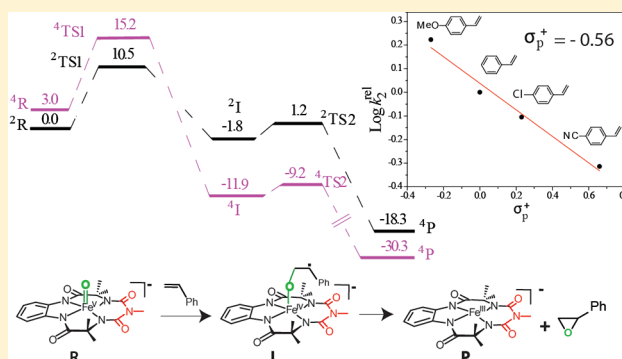


Mechanism of Oxygen Atom Transfer from $\text{Fe}^{\text{V}}(\text{O})$ to Olefins at Room TemperatureKundan K. Singh,[†] Mrityunjay k. Tiwari,[‡] Basab B. Dhar,[†] Kumar Vanka,^{*,‡} and Sayam Sen Gupta^{*,†}[†]Chemical Engineering Division and [‡]Physical and Materials Chemistry Division, CSIR-National Chemical Laboratory, CSIR-National Chemical Laboratory, Pune 411008, India

Supporting Information

ABSTRACT: In biological oxidations, the intermediate $\text{Fe}^{\text{V}}(\text{O})(\text{OH})$ has been proposed to be the active species for catalyzing the epoxidation of alkenes by nonheme iron complexes. However, no study has been reported yet that elucidates the mechanism of direct O-atom transfer during the reaction of $\text{Fe}^{\text{V}}(\text{O})$ with alkenes to form the corresponding epoxide. For the first time, we study the mechanism of O-atom transfer to alkenes using the $\text{Fe}^{\text{V}}(\text{O})$ complex of biuret-modified Fe–TAML at room temperature. The second-order rate constant (k_2) for the reaction of different alkenes with $\text{Fe}^{\text{V}}(\text{O})$ was determined under single-turnover conditions. An 8000-fold rate difference was found between electron-rich (4-methoxystyrene; $k_2 = 216 \text{ M}^{-1} \text{ s}^{-1}$) and electron-deficient (methyl *trans*-cinnamate; $k_2 = 0.03 \text{ M}^{-1} \text{ s}^{-1}$) substrates. This rate difference indicates the electrophilic character of $\text{Fe}^{\text{V}}(\text{O})$. The use of *cis*-stilbene as a mechanistic probe leads to the formation of both *cis*- and *trans*-stilbene epoxides (73:27). This suggests the formation of a radical intermediate, which would allow C–C bond rotation to yield both stereoisomers of stilbene–epoxide. Additionally, a Hammett ρ value of -0.56 was obtained for the para-substituted styrene derivatives. Detailed DFT calculations show that the reaction proceeds via a two-step process through a doublet spin surface. Finally, using biuret-modified Fe–TAML as the catalyst and NaOCl as the oxidant under catalytic conditions epoxide was formed with modest yields and turnover numbers.



INTRODUCTION

The development of a biomimetic oxidation catalyst containing cheap, readily available, and nontoxic metals like Fe is being keenly pursued, but the development of Fe-based complexes that catalyze epoxidation of olefins with high selectivity using inexpensive and environmentally friendly terminal oxidants remains a challenge. The key to such development lies in understanding the mechanism of biological and biomimetic oxidations, especially in identifying metal-based high-valent iron–oxo intermediates and in mapping their reactivity with target substrates.² In biological systems, Fe-containing heme and nonheme centers have both been shown to catalyze the epoxidation reaction. For heme-containing cytochrome P450, the well-established $\text{Fe}^{\text{IV}}(\text{O})$ –porphyrin^{•+} is the active oxidant.³ In nonheme enzymes, the reactive intermediate $\text{Fe}^{\text{V}}(\text{O})(\text{OH})$ has been proposed to catalyze both the epoxidation and the *cis*-dihydroxylation reaction.⁴ These have been shown to be two closely related transformations, and the product outcome can be controlled by addition of additives such as acetic acid.⁵ In contrast, the related $\text{Fe}^{\text{IV}}(\text{O})$ has been shown to be weakly active in catalyzing epoxidation reactions.^{5c} Several nonheme Fe-based complexes catalyze the epoxidation (and related *cis*-hydroxylation reaction) and can be divided into Class A catalysts, such as $[\text{Fe}(\text{TPA})(\text{OTf})_2]$, which preferen-

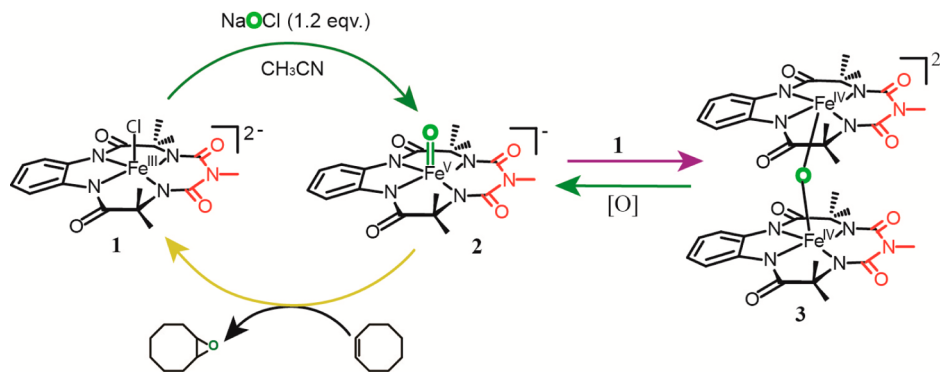
tially carry out epoxidation of electron-rich olefins, and Class B catalysts, such as $[\text{Fe}(6\text{-Me}_3\text{-TPA})(\text{OTf})_2]$, which selectively perform epoxidation of electron-poor olefins like acrylate and fumarate more rapidly than electron-rich olefins.⁶ The $\text{Fe}^{\text{V}}(\text{O})$ intermediate has been proposed to be the active oxidant for Class A catalysts. In 2009, Talsi et al.^{7a} reported the probable involvement of $\text{Fe}^{\text{V}}(\text{O})$ during epoxidation by a nonheme iron catalyst at -70°C on the basis of only EPR measurements (the amount was estimated to be around 15%). The epoxidation rate was estimated by the decay of this $S = 1/2$ species in EPR measurements. However, no direct experiments have been reported yet that characterize the reactivity of $\text{Fe}^{\text{V}}(\text{O})$ intermediate with olefins with varying electronic and steric properties. Given that epoxidation is a synthetically useful and mechanistically important process, such studies would shed light on the reactivity of nonheme iron complexes that catalyze the epoxidation reaction.

We recently reported the stoichiometric formation of $[\text{Fe}^{\text{V}}(\text{O})\text{-(biuret-TAML)}]^-$ complex 2 at room temperature (RT) with NaOCl/*m*-CPBA as an oxidant.^{7b} The reactivity of this $\text{Fe}^{\text{V}}(\text{O})$ for activation of C–H bonds and in photochemical

Received: December 22, 2014

Published: June 8, 2015



Scheme 1. Catalytic Scheme for the Epoxidation of *cis*-Cyclooctene by $[\text{Fe}^{\text{V}}(\text{O})-(\text{biuret-TAML})]^-$ 

water oxidation has been reported.^{7b,8} In this work, we report the reactivity of $[\text{Fe}^{\text{V}}(\text{O})-(\text{biuret-TAML})]^-$ (2) with a wide variety of alkenes. The second-order rate constants derived with alkenes with varying electronic properties indicate the $\text{Fe}^{\text{V}}(\text{O})$ to be an electrophilic oxidant. Using a combination of experimental and theoretical studies (DFT), we propose a detailed mechanism of the epoxidation reaction.

EXPERIMENTAL SECTION

Materials. Biuret-amide-modified Fe-TAML (1) was synthesized as reported by us before.^{9a} Aqueous sodium hypochlorite (reagent grade, Aldrich, available chlorine 4.00–4.99%) was used as received and quantified by iodimetry. Acetonitrile (HPLC grade, Aldrich) was used after passing through an activated neutral alumina column. O¹⁸-enriched (98%) water was procured from Shanghai Research Institute of Chemical Industry, China. Deionized water was used to make all stock solutions of NaOCl for the reaction and kinetic runs. Styrene, 4-chlorostyrene, 4-methoxystyrene, and *cis*-cyclooctene were purchased from Aldrich and distilled before use. *cis*-Stilbene, *trans*-stilbene, norbornene, methyl *trans*-cinnamate, and KPF₆ were purchased from Aldrich and used as received. 4-Cyanostyrene was synthesized by the Wittig reaction,^{9b} and purity was checked by GC. All reactions were carried out without any special precautions under atmospheric condition unless mentioned.

General Instrumentation. UV-vis spectral studies were carried out using an Agilent diode array 8453 spectrophotometer attached with an electrically controlled thermostat. Gas chromatography (GC) was performed on a PerkinElmer Arnel Clarus 500 instrument equipped with a hydrogen flame ionization detector and HP-5 (30 m × 0.32 mm × 0.25 μm) column. Helium was used as carrier gas at a flow rate of 30 mL min⁻¹. GC-MS were performed on an Agilent 5977A mass-selective detector interfaced with an Agilent 7890B GC in similar conditions using a HP-5-MS capillary column (30 m × 0.32 mm × 0.25 μm, J & W Scientific). High-resolution mass spectrometry (HR-MS) was done in a Thermo Scientific Q-Exactive using an electron spray ionization source and an Orbitrap as the analyzer and connected with a C18 column (150 m × 4.6 mm × 8 μm).

Reactivity of $\text{Fe}^{\text{V}}(\text{O})$ (2) toward Alkene Epoxidation. At least three kinetic runs were carried out for each experiment; mean values are reported here. The kinetics were monitored in either the kinetic mode of the spectrophotometer or the scanning spectral kinetics mode using a 1.0 cm quartz cell at 396 nm [Isosbestic points of Fe^{IV} species and Fe^{III}] at 25.0 °C.^{7b,10} All kinetic experiments were carried out in CH₃CN. During kinetic measurements, $\text{Fe}^{\text{V}}(\text{O})$ was prepared by using 1.1 equiv of NaOCl, and substrate was added to it under pseudo-first-order condition (concentration of 2 was from 2×10^{-5} to 1×10^{-4} M, depending upon reactivity of the substrate, and different alkenes concentrations were chosen according to the needs of the experiment, which were from 2×10^{-4} to 1.8×10^{-1} M, see Figure SI 1, Supporting Information). The pseudo-first-order rate constant (k_{obs}) was calculated at the isosbestic wavelength by nonlinear curve fitting $[A_t = A_{\infty} - (A_{\infty} - A_0)e^{(-k_{\text{obs}}t)}]$ and had good agreement in rate

constant value within 10% error. Resulting k_{obs} values correlated linearly with substrate concentration to give second-order rate constant k_2 .

Single-Turnover Reaction. Excess substrate (50 μL, 10^{-1} M) was added to a freshly prepared 500 μL solution of 2 [generated by reaction of 1 (2×10^{-4} M) and NaOCl (2.2×10^{-4} M)] at room temperature (RT). Reaction mixture was stirred for 20–70 min. After completion of the reaction (determined by UV-vis spectroscopy), the products (yield %) were quantified by GC using a calibration curve obtained with authentic epoxides of respective alkene. The products were identified by GC-MS and NMR.

Cyclic Voltammetry. Cyclic voltammetry (CV) was carried out using a BioLogic potentiostat (model VMP-3) in a conventional three-electrode electrochemical cell with glassy carbon as the working electrode, saturated calomel electrode (SCE) as a reference electrode, and platinum foil as a counter electrode. The measurements were carried out with a 0.25 mM solution of 2 in acetonitrile (prepared by addition of 2 equiv of NaOCl into complex 1) with 10 mM KPF₆ as the supporting electrolyte at 0 °C. All peaks were independently calibrated with respect to an internal ferrocene/ferrocenium (Fc/Fc^+) redox couple under identical condition.

Catalytic Reaction. A 200 equiv amount (with respect to complex 1) of aq NaOCl (at pH 11.4) was added to 1 mL of acetonitrile solution containing complex 1 (1×10^{-4} – 1.5×10^{-4} M) and 67–100 equiv of substrate (with respect to complex 1). The reaction was run with stirring for 10, 40, and 70 min for 4-methoxystyrene, stilbene (*cis* and *trans*), and methyl *trans*-cinnamate, respectively. At the end of the reaction, 2 mL of water was added to the reaction mixture and product was extracted in dichloromethane (five times with 2 mL of dichloromethane each time). Collected organic phase solvent was evaporated by purging nitrogen gas, and the volume was adjusted to 500 μL for product quantification by GC.

O¹⁸ Incorporation Experiment. To 200 μL of an acetonitrile solution of 1 (5×10^{-4} M), 1.2 equiv of NaOCl was added, which leads to the formation of $\text{Fe}^{\text{V}}(\text{O})$ (2). H₂O¹⁸ (20 μL) was introduced into the solvent media of species 2, and the solution was allowed to stand approximately 3 h at –22 °C. The HRMS showed 30% incorporation of O¹⁸, leading to the formation of $[\text{Fe}^{\text{V}}(\text{O}^{18})(\text{biuret-TAML})]^-$ m/z 431.0763 (calculated m/z 431.0773). Into two separate sets of the same experiment, 50 μL of a solution of 10^{-1} M *cis*-cyclooctene and methyl *trans*-cinnamate substrate was added to the labeled $\text{Fe}^{\text{V}}(\text{O}^{18})$ solution. HR-MS and GC-MS showed the O¹⁸-labeled corresponding epoxides.

Computational Details. To carry out the mechanistic study, methods based on density functional theory (DFT) have been employed. All minima and transition states reported in this study were fully optimized at the UB3LYP/6-31G*, LANL2DZ (Fe) level of theory¹¹ using the Gaussian 09 suite of quantum-chemical programs.¹² The stationary points on the potential energy surface were characterized by evaluating the vibrational frequencies. The zero-point vibrational energy corrections and thermal corrections were applied to the “bottom-of-the-well” values to obtain values for the Gibbs free energy at 298.15 K. The mechanism was derived

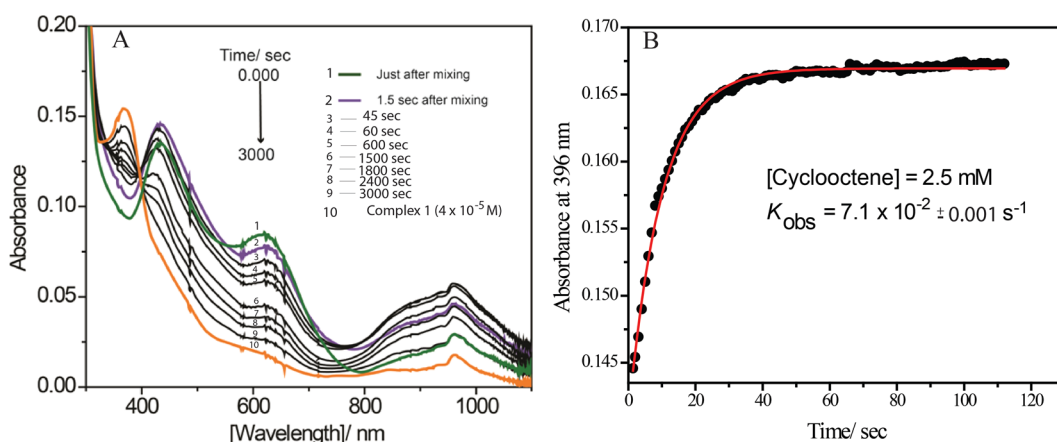
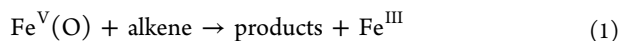


Figure 1. (A) UV-vis spectral changes upon reaction of **2** ($4 \times 10^{-5} \text{ M}$) with *cis*-cyclooctene ($2.5 \times 10^{-3} \text{ M}$); (B) absorbance vs time plot at 396 nm for reaction of **2** ($4 \times 10^{-5} \text{ M}$) with *cis*-cyclooctene ($2.5 \times 10^{-3} \text{ M}$) ((●) experimental data point; (red line) first-order fit according to the equation $[(A_t = A_\infty - (A_\infty - A_0)e^{(-k_{\text{obs}}t)}]$). Reaction was performed at RT in acetonitrile solvent under nitrogen atmosphere.

considering styrene as the representative structure of its derivatives, such as para-substituted styrenes and stilbene. All energies were calculated with respect to the infinitely separated reactants. The products are also considered to be infinitely separated. All values provided in Figure 3 are electronic energies.

RESULTS AND DISCUSSION

Kinetics of *cis*-Cyclooctene Epoxidation under Single-Turnover Condition. Compound **2** was prepared at 25°C from the parent biuret-TAML activator, $(\text{Et}_4\text{N})_2[\text{Fe}^{\text{III}}(\text{Cl})\text{-(biuret-TAML)}]$ (**1**), in CH_3CN by adding equimolar (1.1 equiv) amounts of NaOCl, as reported before. The unprecedented high stability of **2** allowed us to perform extensive kinetic studies in single-turnover condition to ascertain the mechanism of epoxidation using UV-vis spectroscopy at RT (Scheme 1). Initial experiments showed that upon addition of *cis*-cyclooctene ($2.5 \times 10^{-3} \text{ M}$) to a preformed solution of **2** ($4 \times 10^{-5} \text{ M}$), the green color of the reaction mixture immediately changed to brown. A UV-vis scanning kinetics study showed that the starting $\text{Fe}^{\text{V}}(\text{O})$ species changed to the diamagnetic $\mu\text{-oxo-Fe}^{\text{IV}}$ dimer species, which then slowly regenerated the parent Fe^{III} complex **1** (Figure 1A, peak at 379 nm) quantitatively (for complete characterization of $\mu\text{-oxo-Fe}^{\text{IV}}$ dimer species please see ref 7b). The direct conversion of **2** to **1** was not observed in initial spectral scans, since the rate of the comproportionation reaction ($1.0 \times 10^5 \text{ M}^{-1} \text{ s}^{-1}$) between **1** and **2** (eq 2) was faster than the rate of epoxidation ($29 \text{ M}^{-1} \text{ s}^{-1}$; Table 1, entry 8).



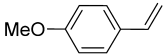
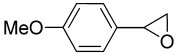
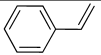
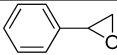
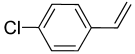
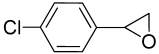
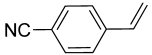
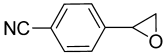
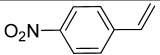


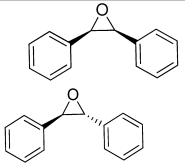
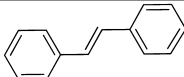
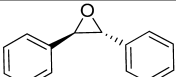
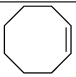
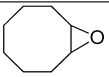
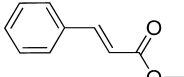
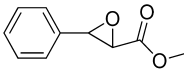

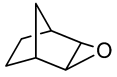
The pseudo-first-order rate constant (k_{obs}) correlated linearly with [*cis*-cyclooctene] (Figure 1B), and the second-order rate constant k_2 ($29 \text{ M}^{-1} \text{ s}^{-1}$) was calculated from the slope of the straight line. After completion of the reaction, product identification was carried out by GC-MS; the results showed that cyclooctene oxide was formed as the major product ($\sim 65\%$). It should be noted that the fast comproportionation between **1** and **2** would allow only 50% of **2** to react with alkenes and yield a maximum of only 50% yield epoxide (with respect to **2**). The higher yields of epoxide observed are due to

the slow reaction of alkenes with the Fe^{IV} dimer (Figure SI 2, Supporting Information) (separately discussed below). Less than 1% of *trans*-cyclooctane-1,2-diol was observed as a side product. Quantification of the epoxide was done by GC. Control experiments with only NaOCl in our experimental conditions showed no formation of cyclooctene oxide.

Kinetics of the Epoxidation of Various Alkenes under Single-Turnover Conditions. To ascertain the mechanism of epoxidation, single-turnover experiments were performed by adding preformed **2** (from 2×10^{-5} to $1 \times 10^{-4} \text{ M}$, depending upon reactivity of the substrate) to various alkenes having varying electronic and steric properties (Table 1) under pseudo-first-order conditions. After completion of the reaction, all products of these single-turnover reactions were identified by GC-MS and then quantified by GC (Figure SI 3, Supporting Information). GC-MS showed exclusive formation of epoxide with moderate yields ($>70\%$) for most alkenes. For the alkenes *trans*-stilbene, norbornene, and *cis*-cyclooctene, the side products formed were identified as benzaldehyde ($<2\%$), *trans*-norbornane-2,3-diol ($<1\%$), and *trans*-cyclooctane-1,2-diol ($<1\%$) respectively. When *cis*-stilbene was used as a substrate, in addition to the formation of *cis*-stilbene oxide (56%), considerable amounts of isomerized products, i.e., *trans*-stilbene oxide (21%), were observed (Table 1, entry 6). When *trans*-stilbene was used as the substrate, *trans*-stilbene oxide was formed exclusively, and no *cis*-stilbene oxide was found (Table 1, entry 7). Additionally, stereochemical retention was also observed for the epoxidation of methyl *trans*-cinnamate. In all reactions, the starting Fe^{III} complex (**1**) was quantitatively regenerated after the single-turnover reaction. To ascertain that the O atom was incorporated into the alkene upon epoxidation from the $\text{Fe}^{\text{V}}(\text{O})$, O^{18} labeling experiments were performed. Epoxidation was carried out on two different alkenes (methyl *trans*-cinnamate, *cis*-cyclooctene) using a mixture of $\text{Fe}^{\text{V}}(\text{O}^{16})$ and $\text{Fe}^{\text{V}}(\text{O}^{18})$ (ratio of 68:32) (Figures SI 4 and 5, Supporting Information). The epoxides obtained after completion of the reaction showed $\sim 30\%$ incorporation of O^{18} into the epoxide, which confirmed that oxygen incorporated into the epoxide was transferred from $\text{Fe}^{\text{V}}(\text{O})$ (Figures SI 6 and 7, Supporting Information).

The kinetics of the reaction was then studied to determine the second-order rate constant k_2 , as described above (Figure SI 1, Supporting Information). The k_2 values obtained for all of

Table 1. Epoxidation of Different Alkenes by $\text{Fe}^{\text{V}}(\text{O})^{\text{a}}$ at RT in CH_3CN under Air

Entry	Substrates ^b	Products	Reaction time / min	$k_2 / \text{M}^{-1} \text{s}^{-1}$	%Yields ^c
1			20	216.0 ± 3.2	74 ± 6
2			50	148 ± 8.1	71 ± 6
3			50	116 ± 4.6	70 ± 6
4			50	72.0 ± 3.7	62 ± 5
5			50	n.d.	66 ± 5
6			50	26.5 ± 0.8	77 ± 4 , (73:27)
7			50	3.1 ± 0.06	81 ± 4
8			30	29.0 ± 3.6	65 ± 5
9			70	0.03 ± 0.001	86 ± 6
10			20	321.0 ± 8.7	78 ± 7

^aConcentration of $\text{Fe}^{\text{V}}(\text{O})$ used to obtain k_2 values was $2 \times 10^{-5} \text{ M}$ (for entries 1 and 10), $4 \times 10^{-5} \text{ M}$ (for entries 2–4 and 8), and $1 \times 10^{-4} \text{ M}$ (for entries 6, 7, and 9). For yield of epoxides under single-turnover conditions, the concentration of $\text{Fe}^{\text{V}}(\text{O})$ was $2 \times 10^{-4} \text{ M}$. ^bConcentration variation of substrates used to obtain k_2 was in the range of 10–100 equiv (for entries 1–4, 6–8, and 10) and 500–1750 equiv (for entry 9) with respect to $\text{Fe}^{\text{V}}(\text{O})$. For obtaining single-turnover yields the substrate concentration used was $1 \times 10^{-2} \text{ M}$. ^cYields of epoxides are with respect to $\text{Fe}^{\text{V}}(\text{O})$.

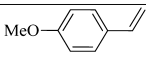
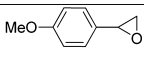
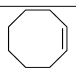
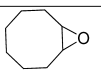
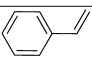
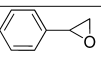
the different alkenes show that the rates of epoxidation of electron-rich substrates were much faster than those of the electron-deficient ones. For example, the k_2 value for 4-methoxystyrene (Table 1, entry 1) was determined to be $216 \text{ M}^{-1} \text{s}^{-1}$, while that of methyl *trans*-cinnamate (Table 1, entry 9) was $0.03 \text{ M}^{-1} \text{s}^{-1}$. This 8000-fold rate difference between electron-rich and electron-deficient substrates indicates that $\text{Fe}^{\text{V}}(\text{O})$ has electrophilic character, reminiscent of nonheme epoxidation catalysts that have been discussed before. The reactivity of the disubstituted alkenes (e.g., cyclooctene, *cis*-stilbene) is much slower than expected, possibly due to the steric crowding of the disubstituted alkenes. The effect of electron-donating and -withdrawing groups on alkenes was explored in more detail by using a series of substituted styrenes. Kinetic studies revealed that styrene with a para-substituted

electron-donating group was more reactive than styrene having a para-substituted electron-withdrawing group (Table 1). For example, k_2 for the epoxidation of *p*-cyanostyrene was determined to be ~ 3 times slower than the rate of *p*-methoxystyrene. We were unable to determine the exact k_2 value of *p*-nitrostyrene, since its strong UV absorption in the 300–400 nm region interfered with the $\text{Fe}^{\text{III/IV}}$ isosbestic point (Figure SI 8, Supporting Information).

Reactivity of μ -Oxo- Fe^{IV} Dimer. The >50% yield of epoxide formation observed in the single-turnover experiments is unlikely because the fast comproportionation between **1** and **2** would only allow 50% of **2** to react with alkenes and yield a maximum of only 50% epoxide (with respect to **2**). The higher yields of epoxide observed are due to the slow reaction of alkenes with the μ -oxo- Fe^{IV} dimer, which was investigated in

the reaction of 4-methoxystyrene and *cis*-cyclooctene with μ -oxo- Fe^{IV} dimer (Table 2). The μ -oxo- Fe^{IV} dimer was

Table 2. Epoxidation of Alkenes by μ -Oxo- Fe^{IV} Dimer^a at RT in CH_3CN Solvent under Air

Substrates ^b	Products	$k_2/\text{M}^{-1}\text{s}^{-1}$
		4.4 ± 0.2
		0.2 ± 0.01
		0.8 ± 0.02

^aConcentration of μ -oxo- Fe^{IV} dimer was 1×10^{-5} M for reaction with 4-methoxystyrene and 2×10^{-5} M for reaction with *cis*-cyclooctene and styrene. ^bConcentration of substrates was in range from 2.5×10^{-4} to 4×10^{-3} M.

synthesized by addition of 0.5 equiv of NaOCl in complex **1**, which has characteristic UV-vis spectra similar to the previously reported μ -oxo- Fe^{IV} dimer (which is formed upon equimolar amounts of **1** in **2**; characterized by ^1H NMR and EPR).^{7b,10} The μ -oxo- Fe^{IV} dimer species reacts with alkenes to form a corresponding epoxide. For example, in the reaction of μ -oxo- Fe^{IV} dimer with 4-methoxystyrene, *cis*-cyclooctene and styrene corresponding epoxide were observed with a rate of reaction more than 50-fold slower than the corresponding reaction with $\text{Fe}^{\text{V}}(\text{O})$, **2**. Although we do not have any conclusive evidence of the mechanism of this reaction, we believe that the μ -oxo- Fe^{IV} dimer disproportionates into $\text{Fe}^{\text{V}}(\text{O})$ (**2**) and Fe^{III} complex (**1**), after which the $\text{Fe}^{\text{V}}(\text{O})$ reacts with alkenes to form the epoxide product (Scheme SI 1, Supporting Information). Two scenarios are possible: (1) binding of alkene to the μ -oxo- Fe^{IV} dimer leads to the disproportionation reaction, after which the $\text{Fe}^{\text{V}}(\text{O})$ reacts, or (2) the μ -oxo- Fe^{IV} dimer exists in an equilibrium with the $\text{Fe}^{\text{V}}(\text{O})$ and Fe^{III} complex. The reaction of the alkene with $\text{Fe}^{\text{V}}(\text{O})$ leads to more disproportionation of the dimer, leading to the formation of more $\text{Fe}^{\text{V}}(\text{O})$, which reacts with the alkene until all of it is converted to the starting $\text{Fe}(\text{III})$ complex. If the first hypothesis is correct, a saturation in the k_{obs} values of the reaction of the μ -oxo- Fe^{IV} dimer with the substrate should be

observed at high substrate concentration. However, no saturation was observed for the k_{obs} with styrene/methoxystyrene with up to 750 equiv of the substrate, implying that the substrate-mediated disproportionation was probably not occurring. Further, the reaction of μ -oxo- Fe^{IV} dimer with 4-methoxystyrene in the presence of different amounts of parental Fe^{III} complex **1** showed reduction in reaction rates with increasing amounts of **1** into the reaction mixture. The plot of reaction rate vs amount of Fe^{III} (**1**) in reaction mixture shows a good fit into the kinetic model

$$\text{rate} = \frac{k_1 k_2 [\mu\text{-oxo-Fe}^{\text{IV}} \text{ dimer}] [\text{substrate}]}{k_{-1} [\text{Fe}^{\text{III}}] + k_2 [\text{substrate}]}$$

Using a k_2 value of $216 \text{ M}^{-1} \text{ s}^{-1}$ (as earlier determined for methoxystyrene under single-turnover conditions), k_1 and k_{-1} were determined to be 0.024 and 24 620, respectively. (Figure SI 9, Supporting Information)

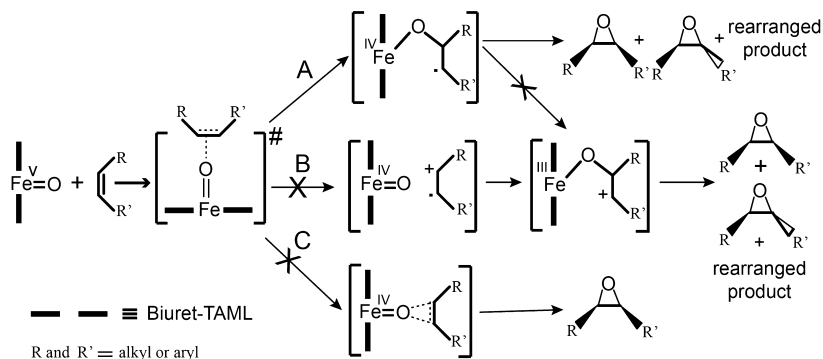
Possible Mechanisms of Epoxidation. Three possible mechanisms for initial attack of "O" into the alkene during the epoxidation reaction have been proposed:

- (1) the transfer of oxygen into the alkene by a concerted process (Scheme 2, path C), as is known for the epoxidation of alkenes by the enzyme cytochrome P450,^{2a,3a,13}
- (2) generation of the acyclic carbocation radical through one-electron transfer¹⁴ (Scheme 2, path B), and
- (3) radical intermediate formation via electrophilic attack of $\text{Fe}^{\text{V}}(\text{O})$ upon alkene with concomitant C–O bond formation¹⁵ (Scheme 2, path A).

Understanding the pathway is important, since the product selectivity during the epoxidation reaction depends upon the mechanism through which the reaction proceeds. For example, both the second and the third pathways have been observed for synthetic Fe–porphyrin complexes as well as Mn–salen complexes.¹⁶ In fact, it has been shown that the reaction pathway between **2** and **3** can be manipulated by varying the axial ligands in synthetic iron porphyrins.¹⁷ The other possibility for the catalytic reaction is the axial coordination of the second equivalent of NaOCl to the $\text{Fe}^{\text{V}}(\text{O})$, resulting in the formation of $\text{Fe}^{\text{V}}(\text{O})\text{OCl}$, as observed in Fe–porphyrins. We exclude this possibility since the addition of excess NaOCl to complex **2** does not show any change in the UV-vis spectra of the starting $\text{Fe}^{\text{V}}(\text{O})$. All possible pathways are schematically shown below (Scheme 2).

Epoxidation by Pathway C. To probe experimentally if the epoxidation reactions by $\text{Fe}^{\text{V}}(\text{O})$ occurs via pathway C, the

Scheme 2. Detailed Mechanistic Scheme for the Epoxidation of Alkenes by $[\text{Fe}^{\text{V}}(\text{O})-(\text{biuret-TAML})]^-$



substrate *cis*-stilbene was used as a mechanistic probe, as has been shown by Bruce et al. in the case of electron-deficient cytochrome P-450 model complexes (e.g., *meso*-tetrakis(2,6-dichlorophenyl)porphinato-oxo-iron(IV), [(C₁₈TPP⁺•)-Fe^{IV}(O)]).^{14b,18} If *cis*-stilbene leads to the exclusive formation of *cis*-stilbene oxide, it indicates the predominance of a concerted mechanism. In contrast, if a mixture of both *cis*- and *trans*-configured epoxide is observed, it would point to the formation of a radical intermediate that would allow C–C bond rotation to give the stereoisomers. In the epoxidation of *cis*-stilbene with Fe^V(O), formation of both *cis*- and *trans*-stilbene epoxide is observed (ratio 73:27); hence, the pathways via a concerted mechanism look unlikely (Path C in Scheme 2). Further, DFT calculations discussed below also show that the epoxidation of styrene by Fe^V(O) complexes are indeed nonconcerted processes.

Epoxidation via Pathways A and B. The loss of stereochemistry during the epoxidation of *cis*-stilbene can be explained by invoking the formation of a radical intermediate (Scheme 2, Path A or B). To distinguish between pathway A and pathway B, we looked carefully at the rates of epoxidation with various substituted alkenes. It has been shown that for epoxidation reactions operating via pathway B, i.e., the rate-determining step (RDS) being one-electron oxidation, the second-order rate constants vary linearly with the ionization potential (IP) of alkenes.¹⁹ In our study of alkene epoxidation by Fe^V(O), the plot of k_2 vs IP of alkenes does not show any linearity (Figure SI 10, Supporting Information).

DFT studies also point to the fact that pathway B is not followed during the epoxidation process. The calculations show that the epoxidation of styrene by Fe^V(O) complexes **2** is indeed a nonconcerted process, with C–O bond formation being the rate-determining step (Figure 3 and Table SI 1, Supporting Information), followed by a very low barrier ring-closing step. This corresponds to pathway A in Scheme 2. The existing literature on analogous systems suggests similar observations, which were further supported by DFT studies.^{3c,18,20} For investigating pathway B (see Scheme 2), we looked at the correlation diagram of the ionization potential of the substrates versus the experimentally measured second-order rate constants (Figure SI 10, Supporting Information). No correlation between the ionization potential and the rate of reaction was obtained, which indicates that one-electron oxidation of the styrene coupled with one-electron reduction of the monoanionic Fe^V(O) complex is unlikely. This is in contrast to the epoxidation catalyzed by Mn and Cr porphyrin catalysts, in which the second-order rate constants strongly correlated to the $E_{1/2}$ of the substrates.^{18,19} Thermodynamic analysis of the epoxidation of olefins by **2** precludes the involvement of the one-electron-reduced Fe^{IV}(O) as the active species during the O-atom transfer leading to formation of the C–O bond. First, the free energy of activation during the epoxidation reaction was determined from the second-order rate constants. This was compared to the standard free energies required for the formation of a one-electron-oxidized alkene, i.e., Fe^V(O) + alkene \rightleftharpoons Fe^{IV}(O) + alkene^{•+}. (The redox potential of Fe^V/Fe^{IV} was determined by performing cyclic voltammetry experiments with chemically synthesized Fe^V(O); see the Experimental Section and Figure SI 11, Supporting Information). The analysis shows that, for several alkenes, the free energy of the one-electron oxidation of alkenes by Fe^V(O) exceeds that of the free energy of the transition state during the epoxidation of alkenes by Fe^V(O) (Table 3), thereby

precluding the role of Fe^{IV}(O) as the active species during C–O bond formation.

Table 3. Calculated Values of the Free Energy of Formation of the Transition State (ΔG^\ddagger) and Standard Free Energy (ΔG°) for the One-Electron Transfer in the Transition State during the Reaction of Fe^V(O) with Alkene at 25 °C in Acetonitrile^a

substrate	$\log k_2$ (M ⁻¹ s ⁻¹)	ΔG^\ddagger (kJ mol ⁻¹)	$E_{1/2}$ (V, SCE)	ΔG° (kJ mol ⁻¹)
norbornene	2.51	47.5	1.90	85.9
styrene	2.17	49.5	1.95	90.7
4-chlorostyrene	2.06	50.1	1.76	72.4
4-cyanostyrene	1.86	51.3	2.05	100.3
<i>cis</i> -cyclooctene	1.54	53.1	2.03	98.4

^a $\Delta G^\ddagger = -RT \ln (k_2 h / kT)$; $\Delta G^\circ = -nF(P_1 - P_2)$, where $n = 1$, $P_1 = E_{1/2}$ (V, SCE) of substrates oxidation, $P_2 = E_{1/2}$ (V, SCE) of Fe^V(O) reduction = 1.01, $F = 96485$ C mol⁻¹, $T = 298$ K, $R = 8.314$ J K⁻¹ mol⁻¹, $k = 1.38 \times 10^{-23}$ J K⁻¹, $h = 6.6 \times 10^{-34}$ J s.

To investigate this further, a geometry optimization of the cationic styrene and the dianionic Fe^{IV}(O) complex was performed in the solvent phase, using the conductor like polarization continuum model (CPCM) method²¹ and with acetonitrile (dielectric constant, $\epsilon = 35.688$) as the solvent. The free energy difference between the obtained ionic species and the rate-determining transition state (RDTS) of pathway A (in this case, also optimized with solvent corrections for the purpose of comparison) was calculated to be 13.0 kcal/mol (Table SI 2, Supporting Information). The calculated free energy of the reaction leading to the formation of the ionic intermediates in pathway B was endergonic by 34.4 kcal/mol (Table SI 2, Supporting Information), which further indicates its unlikelihood.

To understand the effect of the electronic environment associated with the substituent on styrene, different para-substituted styrene derivatives with electron-donating substituents displayed enhanced second-order rate constant (k_2) values when compared to electron-withdrawing para substituents (Table 1). The k_2^{rel} ($k_2^{\text{rel}} = k_2^{\text{X}}/k_2^{\text{H}}$) value for styrene and its analogue was used for linear free energy correlation analysis (Figure 2), and a Hammett ρ value of -0.56 was obtained. The relatively small value of ρ indicated the buildup of partial positive charge on the olefinic carbon in the transition state. However, previous studies showed that the rate-limiting carbocation formations via electrophilic additions to substituted styrenes are associated with much more negative ρ values [i.e., -3.58 (hydration) and -4.8 (bromination)].²² When the barrier heights for pathway A obtained from the DFT calculations were compared for styrene and *p*-chlorostyrene, it was seen that the barrier height for the *p*-chlorostyrene case was higher by 1.9 kcal/mol than for styrene (10.5 kcal/mol for styrene and 12.4 kcal/mol for *p*-chlorostyrene; Tables SI 1 and 3, Supporting Information). This observation indicates that pathway A most likely represents the actual epoxidation mechanism, and therefore, the direction of the flow of electrons inside the styrene substrates during the reaction occurs from the phenyl ring to the CH₂=CH— group. To further investigate the effect of the solvent and the Hammett-type behavior of the styrene derivatives on the rate-determining barriers (RDB), the RDB were calculated using the conductor

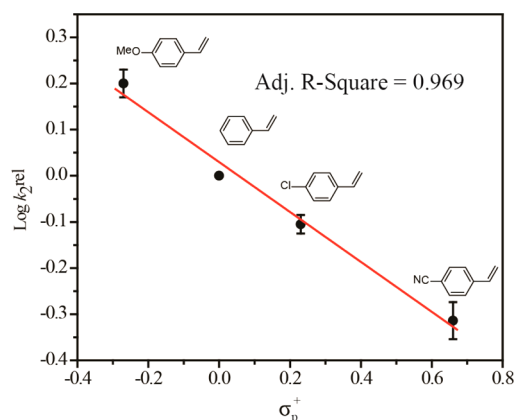


Figure 2. Hammett plots of $\log k_2^{\text{rel}}$ against $\text{para-}\sigma^+$ for the epoxidation of styrenes and its para-substituted derivatives by $\text{Fe}^{\text{V}}(\text{O})$ at RT in CH_3CN . Hammett value ρ is -0.56 ; $k_2^{\text{rel}} = k_2^{\text{X}}/k_2^{\text{H}}$, where k_2^{X} and k_2^{H} are second-order rate constants for para-substituted styrene and styrene, respectively.

polarized continuum model (CPCM) in acetonitrile ($\epsilon = 35.688$) for 4-methoxystyrene, styrene, and 4-chlorostyrene substrates. The obtained result followed the experimental trend, i.e., the barriers are obtained in the following order: 4-chlorostyrene (12.7 kcal/mol) > styrene (9.2 kcal/mol) > 4-methoxystyrene (8.8 kcal/mol, see Table SI 4, Supporting Information).

Understanding the α and β Pathways during Styrene Epoxidation. Depending upon the mode of attack on the oxo group by the substrate styrene, two possible pathways for epoxidation are possible for pathway A: the α pathway and the β pathway (Figure 3A and 3B). The α pathway entails the

approach of the α carbon of styrene onto the oxo group of the catalyst, whereas the β pathway involves the attack of the β carbon onto the catalyst. The complete energy profile suggests that the β attack is energetically more favorable (see Figure 3B). The reactive species formed by the β attack is more stable due to the extended conjugation of the phenyl ring.

For the β pathway, there are again two possibilities that need to be investigated: the reaction could occur on the doublet surface or on the quartet surface. As Figure 3 indicates, the reactant $\text{Fe}^{\text{V}}(\text{O})$ complex is more stable as a doublet than a quartet by 3.0 kcal/mol (Table SI 5, Supporting Information). This suggests that the species would exist predominantly in the doublet state, a result that is supported by the experimental observations (the EPR of $\text{Fe}^{\text{V}}(\text{O})$ shows resonances characteristic of $S = 1/2$ species).^{7b} At the intermediate stage, after the crossing of the first barrier, the calculations show that the quartet adduct structure is more stable than the doublet, by 10.2 kcal/mol (Table SI 1, Supporting Information). While this suggests a thermodynamic incentive for the system to convert from the doublet to the quartet at the intermediate stage, the barrier for the subsequent reaction is only 3.0 kcal/mol on the doublet surface, which indicates that the reaction would most likely proceed in the forward direction on the doublet surface. It has been noted in the past that while the spin-flip barrier is expected to be low, it is unlikely that the spin flip would compete with the forward reaction process for reactions having forward barriers less than 5.0 kcal/mol.²³ Hence, the reaction would proceed to its end on the doublet surface and lead to the formation of the doublet product ($S = 1/2$). Subsequent to this, with no further reaction occurring, this kinetically obtained product can convert to the quartet product ($S = 3/2$), which is 12.0 kcal/mol lower in energy (see Table SI 1, Supporting

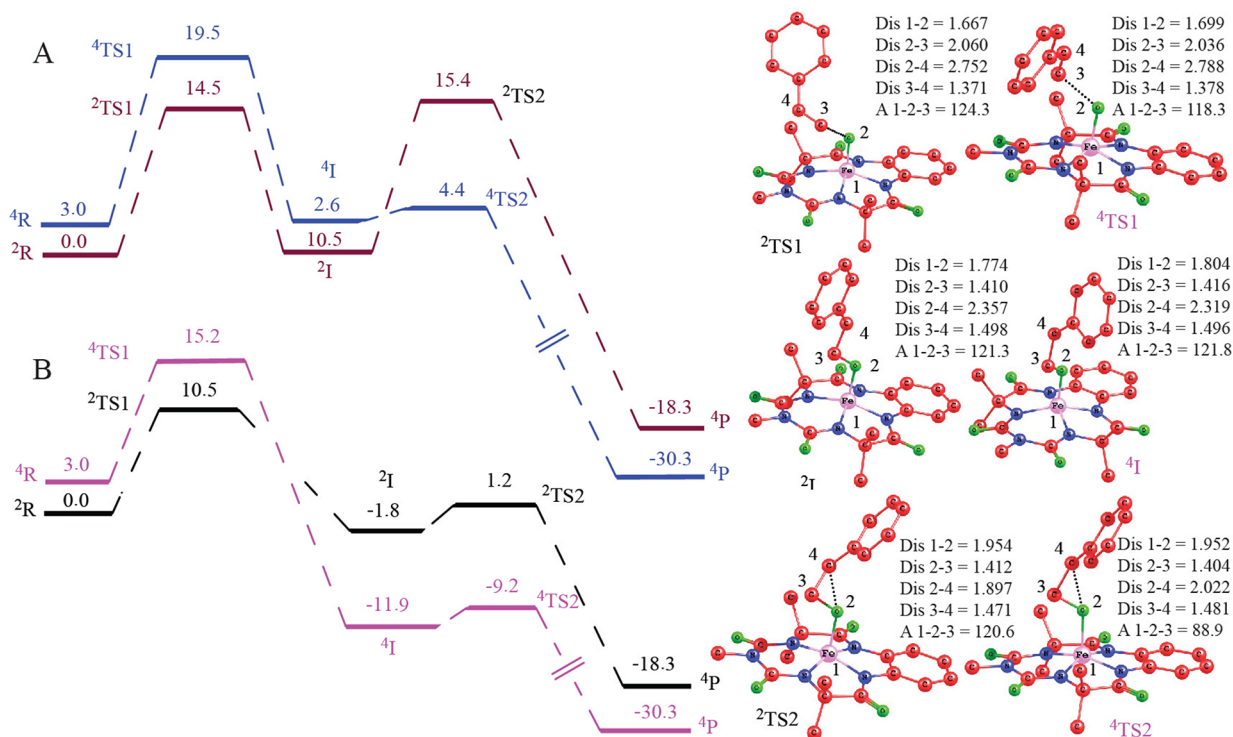


Figure 3. Gas-phase energy profile with optimized geometries of the intermediates and transition states for the epoxidation of styrene by 2 at the UB3LYP/6-31G*, LANL2DZ (Fe) level of theory from doublet and quartet surfaces for the (A) α and (B) β pathway (Dis and A denote distance and angles, respectively; superscripts 2 and 4 represent geometries in the doublet and quartet spin states).

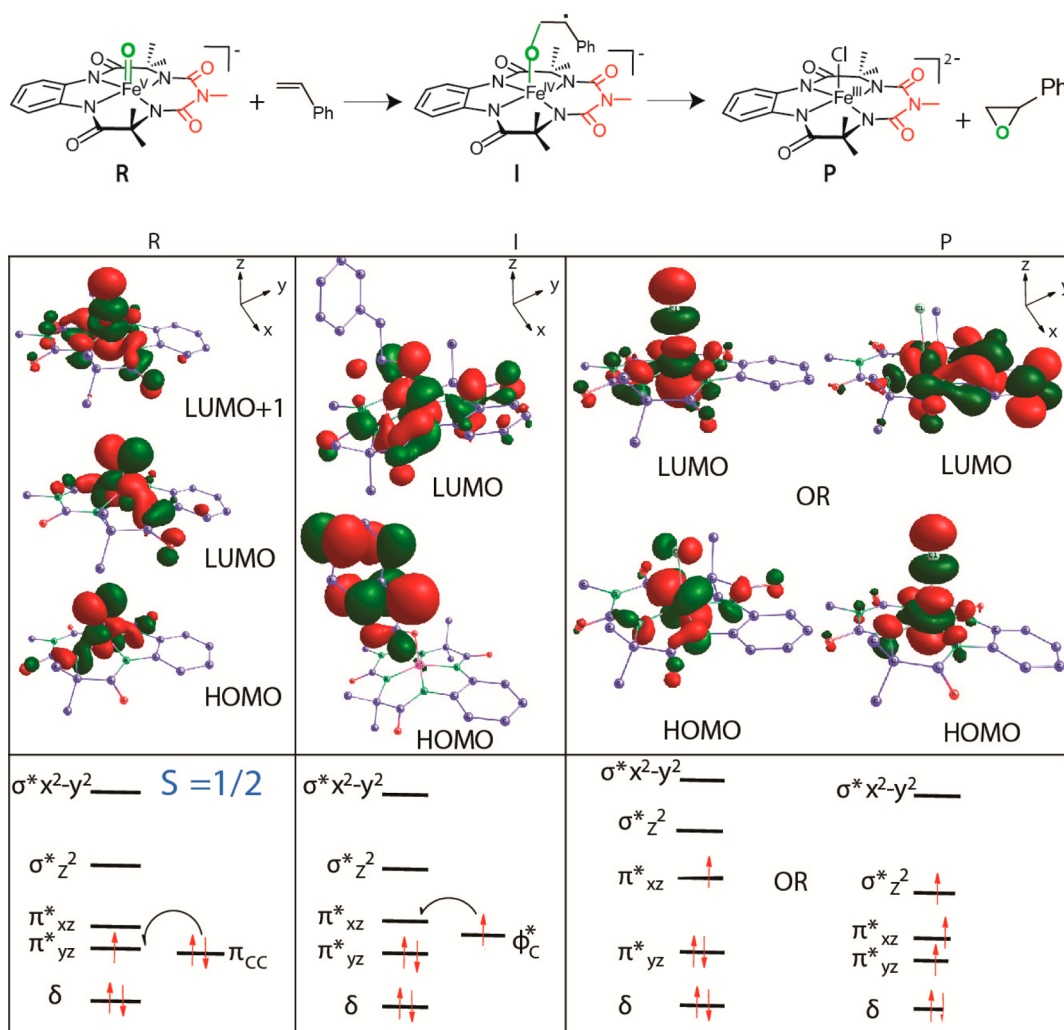


Figure 4. Molecular orbital pictures of the HOMO and LUMO of reactant, intermediate, and product, and orbital occupancy for styrene epoxidation by $\text{Fe}^{\text{V}}(\text{O})$ at the ROB3LYP/6-31G*, LANL2DZ (Fe) level of theory in the gas phase.

Information, and Figure 3B). Hence, the calculations predict a reaction occurring on the doublet surface and leading to the formation of a final quartet product: a result that matches the experimental observation that the final product is a quartet.

Molecular Mechanism of Epoxidation by $\text{Fe}^{\text{V}}(\text{O})$.

Figure 4 shows the frontier orbitals obtained from the DFT calculations for the styrene substrate. As mentioned in the previous section, the reaction would occur on the doublet surface, with the quartet finally being obtained as the thermodynamic product at the end of the reaction. Parts R and I of Figure 4 show the MOs corresponding to the reactant and the intermediate Fe complexes on the doublet surface. The HOMO in the intermediate doublet geometry is seen to be localized on the styrene. Part P shows the MOs obtained for the kinetic doublet product as well as for the thermodynamic quartet product. As also indicated in Figure SI 12, Supporting Information, the energy of the HOMO in the quartet structure is 3.9 kcal/mol lower than the energy of the HOMO in the doublet. According to the “HOMO rule”, the more stable of two structures of a given species is the one whose HOMO is at a lower energy.²⁴ This explains why the quartet structure is more stable than the doublet and, therefore, why the final product of the reaction is a quartet.

Catalytic Activity. Quantitative regeneration of Fe^{III} (**1**) after the single-turnover reaction gave us an opportunity to study the epoxidation reaction in the catalytic condition. The catalytic epoxidation at RT in CH_3CN under air was performed with excess NaOCl (adjusted to pH 11.4). Different olefins (such as 4-methoxystyrene, *trans*-methyl cinnamate, and *trans*-stilbene) were used for the catalytic condition. To optimize reaction conditions, the influence of catalyst concentration was studied in the epoxidation of *cis*-stilbene, *trans*-stilbene, and methyl *trans*-cinnamate in the presence of catalyst **1**. It was observed that the increase in catalyst loading (1–1.5%) leads to faster conversion and greater formation of epoxide due to the increase in the reaction rate (see Figure SI 13, Supporting Information). When the catalyst loading was <1%, less conversion was observed. If the reactions were performed under exclusion of dioxygen, the conversion and yield of epoxide were unaffected; this indicates that molecular oxygen did not have any role in the formation of epoxide. The products formed under optimized reaction conditions are shown in Table 4. Under our reaction condition, side products included *trans*-diol and aldehydes, but the amounts were less than 5% of the epoxide. $\text{PhCH}_2\text{C}(\text{O})\text{Ph}$ was also identified as a side product during the epoxidation of the *cis*/*trans*-stilbene reactions. In the case of 4-methoxystyrene,

Table 4. Summary of the Catalytic Epoxidation^a of Different Alkenes by 1 at RT in CH₃CN under Air

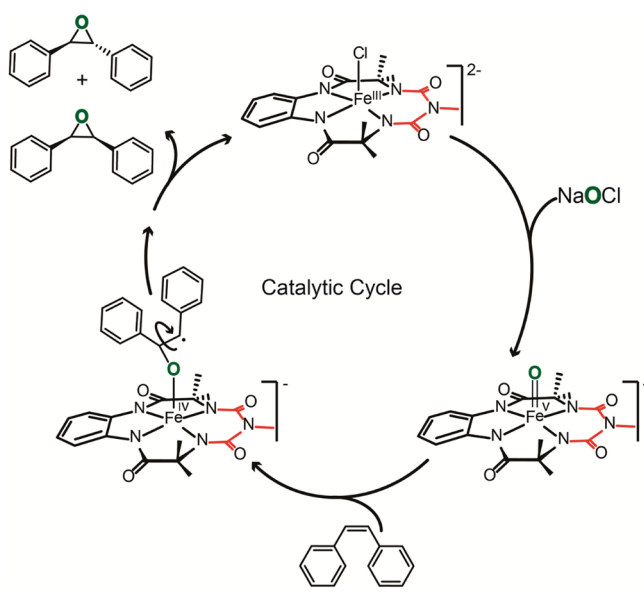
alkene	conversion (%)	yield ^c (%) / epoxide (reaction time)
4-methoxystyrene ^a	74	79 (10 min)
cis-stilbene ^b	97	86 (40 min)
trans-stilbene ^a	99	89 (40 min)
methyl trans-cinnamate ^b	95	90 (70 min)

^aCatalyst 1 (1 × 10⁻⁴ M):NaOCl (2 × 10⁻² M):Substrates (1 × 10⁻² M) = 1:200:100. ^bCatalyst 1 (1.5 × 10⁻⁴ M):NaOCl (3 × 10⁻² M):Substrates (1 × 10⁻² M) = 1.5:300:67. ^cYield of epoxides is with respect to alkenes consumed during the reaction (5% error).

the increase in reaction time leads to increased conversion of alkene but with reduced yield of epoxide. Several unidentified side products were observed during this reaction.

CONCLUSION

A mechanism has been proposed for the epoxidation of olefins by Fe^V(O) (see Scheme 3). Using a combination of

Scheme 3. Proposed Catalytic Cycle for Epoxidation with Complex 1 and NaOCl

experiments and theoretical calculations, we show that the epoxidation proceeds via generation of a radical intermediate through an electrophilic attack on the alkene (Scheme 2, path A). This is followed by a very fast (low-barrier) ring-closing step. There is an 8000-fold rate difference between electron-rich and electron-deficient substrates, which indicates the electrophilic character of Fe^V(O), and is reminiscent of Class A Fe-based epoxidation catalysts. DFT calculations suggest that the reaction proceeds via a two-step process and that both involve a doublet spin surface. We also show that the epoxidation can be carried out in a catalytic manner with modest yields and turnover numbers. Currently, we are studying the deactivation pathways of the catalytic reaction to try to develop more robust catalytic systems.

ASSOCIATED CONTENT

Supporting Information

Detailed kinetic data, gas chromatography data for product formation, HRMS of Fe^V(O); details of DFT calculations are also provided. The Supporting Information is available free of charge on the ACS Publications website at DOI: 10.1021/acs.503053q.

AUTHOR INFORMATION

Corresponding Authors

*E-mail: k.vanka@ncl.res.in.

*E-mail: ss.sengupta@ncl.res.in.

Author Contributions

All authors have contributed to the writing of the manuscript and approved its final version.

Notes

The authors declare no competing financial interest.

ACKNOWLEDGMENTS

S.S.G. acknowledges DST, New Delhi (SERB, EMR/2014/000106) for funding. K.K.S. and M.K.T. acknowledge CSIR (Delhi) for a fellowship. B.B.D. also acknowledges CSIR for a SRA position.

REFERENCES

- (1) (a) Lane, B. S.; Burgess, K. *Chem. Rev.* **2003**, *103*, 2457. (b) Que, L., Jr. *Acc. Chem. Res.* **2007**, *40*, 493.
- (2) (a) Ostović, D.; Bruice, T. C. *Acc. Chem. Res.* **1992**, *25*, 314. (b) Stephenson, N. A.; Bell, A. T. *J. Am. Chem. Soc.* **2005**, *127*, 8635. (c) Traylor, T. G.; Miksztal, A. R. *J. Am. Chem. Soc.* **1989**, *111*, 7443. (d) Que, L., Jr.; Tolman, W. B. *Nature* **2008**, *455*, 333.
- (3) (a) Fruetel, J. A.; Collins, J. R.; Camper, D. L.; Loew, G. H.; Ortiz de Montellano, P. R. *J. Am. Chem. Soc.* **1992**, *114*, 6987. (b) Vaz, A. D. N.; McGinnity, D. F.; Coon, M. J. *Proc. Natl. Acad. Sci. U.S.A.* **1998**, *95*, 3555. (c) de Kumar, D.; Visser, S. P.; Shaik, S. *Chem.—Eur. J.* **2005**, *11*, 2825. (d) Groves, J. T.; Myers, R. S. *J. Am. Chem. Soc.* **1983**, *105*, 5791. (e) Song, W. J.; Ryu, Y. O.; Song, R.; Nam, W. J. *Biol. Inorg. Chem.* **2005**, *10*, 294. (f) Fusii, H. *Coord. Chem. Rev.* **2002**, *226*, 51.
- (4) (a) Moelands, M. A. H.; Nijse, S.; Folkertsma, E.; de Bruin, B.; Lutz, M.; Spek, A. L.; Klein Gebbink, R. J. M. *Inorg. Chem.* **2013**, *52*, 7394. (b) Tiwa, T.; Nakada, M. *J. Am. Chem. Soc.* **2012**, *134*, 13538. (c) Feng, Y.; England, J.; Que, L., Jr. *ACS Catal.* **2011**, *1*, 1035. (d) Krebs, C.; Fujimori, D. G.; Wals, C. T.; Bollinger, J. M. *Acc. Chem. Res.* **2007**, *40*, 484.
- (5) (a) Ballesté, R. M.; Que, L., Jr. *J. Am. Chem. Soc.* **2007**, *129*, 15964. (b) Ye, W.; Ho, D. M.; Friedle, S.; Palluccio, T. D.; Rybak-Akimova, E. V. *Inorg. Chem.* **2012**, *51*, 5006. (c) Suh, Y.; Seo, M. S.; Kim, K. M.; Kim, Y. S.; Jang, H. G.; Tosha, T.; Kitagawa, T.; Kim, J.; Nam, W. J. *Inorg. Biochem.* **2006**, *100*, 627.
- (6) (a) Fujita, M.; Costas, M.; Que, L., Jr. *J. Am. Chem. Soc.* **2003**, *125*, 9912. (b) Chen, K.; Costas, M.; Kim, J.; Tipton, A. K.; Que, L., Jr. *J. Am. Chem. Soc.* **2002**, *124*, 3026.
- (7) (a) Lyakin, O. Y.; Bryliakov, K. P.; Britovsek, G. J. P.; Talsi, E. P. *J. Am. Chem. Soc.* **2009**, *131*, 10798. (b) Ghosh, M.; Singh, K. K.; Panda, C.; Weitz, A.; Hendrich, M. P.; Collins, T. J.; Dhar, B. B.; Sen Gupta, S. *J. Am. Chem. Soc.* **2014**, *136*, 9524.
- (8) (a) Panda, C.; Debgupta, J.; Diaz Diaz, D.; Singh, K. K.; Sen Gupta, S.; Dhar, B. B. *J. Am. Chem. Soc.* **2014**, *136*, 12273. (b) Singh, K. K.; Tiwari, K. M.; Ghosh, M.; Panda, C.; Weitz, A.; Hendrich, M. P.; Dhar, B. B.; Sen Gupta, S. *Inorg. Chem.* **2015**, *54*, 1535.
- (9) (a) Panda, C.; Ghosh, M.; Panda, T.; Banerjee, R.; Sen Gupta, S. *Chem. Commun.* **2011**, *47*, 8016. (b) Wittig, G.; Schoellkopf, U. *Organic Syntheses*; Wiley & Sons: New York, 1973; Collect. Vol. V, p 751. Procedure: Methyltriphenylphosphonium bromide (1.1 equiv) was dissolved in dry THF (25 mL) under inert condition, and to it *n*-butyllithium (1.2 equiv) was added dropwise. It formed a yellow-

colored solution. Then after 1 h of stirring the reaction solution at 0 °C, 4-cyanobenzaldehyde (1 g) was added. The reaction was stirred overnight; then solvent was evaporated by a rotary evaporator. Crude product was adsorbed over silica, and compound was separated by column chromatography.

(10) Kundu, S.; Thompson, J. V. K.; Ryabov, A. D.; Collins, T. J. *J. Am. Chem. Soc.* **2011**, *133*, 18546.

(11) (a) Perdew, J. P.; Chevary, S. H.; Vosko, K. A.; Jackson, K. A.; Pederson, M. R.; Singh, D. J.; Fiolhais, C. *Phys. Rev. B* **1992**, *46*, 6671. (b) Perdew, J. P.; Chevary, S. H.; Vosko, K. A.; Jackson, K. A.; Pederson, M. R.; Singh, D. J.; Fiolhais, C. *Phys. Rev. B* **1993**, *48*, 4978. (c) Perdew, J. P.; Burke, K.; Wang, Y. *Phys. Rev. B* **1996**, *54*, 16533. (d) Adamo, C.; Barone, V. *J. Chem. Phys.* **1998**, *108*, 664. (e) Becke, A. D. *J. Chem. Phys.* **1993**, *98*, 5648. (f) Lee, C.; Yang, W.; Parr, R. G. *Phys. Rev. B* **1988**, *37*, 785. (g) Roothan, C. C. *J. Rev. Mod. Phys.* **1951**, *23*, 69. (h) McWeeny, R.; Dierksen, G. *J. Chem. Phys.* **1968**, *49*, 4852. (i) Pople, J. A.; Nesbet, R. K. *J. Chem. Phys.* **1954**, *22*, 571.

(12) Frisch, M. J.; Trucks, G. W.; Schlegel, H. B.; Scuseria, G. E.; Robb, M. A.; Cheeseman, J. R.; Scalmani, G.; Barone, V.; Mennucci, B.; Petersson, G. A.; Nakatsuji, H.; Caricato, M.; Li, X.; Hratchian, H. P.; Izmaylov, A. F.; Bloino, J.; Zheng, G.; Sonnenberg, J. L.; Hada, M.; Ehara, M.; Toyota, K.; Fukuda, R.; Hasegawa, J.; Ishida, M.; Nakajima, T.; Honda, Y.; Kitao, O.; Nakai, H.; Vreven, T.; Montgomery, J. A., Jr.; Peralta, J. E.; Ogliaro, F.; Bearpark, M.; Heyd, J. J.; Brothers, E.; Kudin, K. N.; Staroverov, V. N.; Kobayashi, R.; Normand, J.; Raghavachari, K.; Rendell, A.; Burant, J. C.; Iyengar, S. S.; Tomasi, J.; Cossi, M.; Rega, N.; Millam, J. M.; Klene, M.; Knox, J. E.; Cross, J. B.; Bakken, V.; Adamo, C.; Jaramillo, J.; Gomperts, R.; Stratmann, R. E.; Yazyev, O.; Austin, A. J.; Cammi, R.; Pomelli, C.; Ochterski, J. W.; Martin, R. L.; Morokuma, K.; Zakrzewski, V. G.; Voth, G. A.; Salvador, P.; Dannenberg, J. J.; Dapprich, S.; Daniels, A. D.; Farkas, Ö.; Foresman, J. B.; Ortiz, J. V.; Cioslowski, J.; Fox, D. J. *Gaussian 09*, revision B.01; Gaussian, Inc.: Wallingford, CT, 2009.

(13) Groves, J. T.; Watanabe, Y. *J. Am. Chem. Soc.* **1986**, *108*, 507.

(14) (a) Collman, J. P.; Kodadek, T.; Brauman, J. I. *J. Am. Chem. Soc.* **1986**, *108*, 2588. (b) Castellino, A. J.; Bruice, T. C. *J. Am. Chem. Soc.* **1988**, *110*, 158.

(15) (a) Groves, J. T.; Kruper, W. J., Jr.; Haushalter, R. C. *J. Am. Chem. Soc.* **1980**, *102*, 6375. (b) Guengerich, F. P.; Macdonald, T. L. *Acc. Chem. Res.* **1984**, *17*, 9. (c) Castellino, A. J.; Bruice, T. C. *J. Am. Chem. Soc.* **1988**, *110*, 1313.

(16) (a) Srinivasan, K.; Michaud, P.; Kochi, J. K. *J. Am. Chem. Soc.* **1986**, *108*, 2309. (b) Yoon, H.; Burrows, C. J. *J. Am. Chem. Soc.* **1988**, *110*, 4087. (c) Zhang, W.; Loebach, J. L.; Wilson, S. R.; Jacobsen, E. N. *J. Am. Chem. Soc.* **1990**, *112*, 2801.

(17) (a) Cussó, O.; Bosch, I. G.; Ribas, X.; Fillol, J. L.; Costas, M. *J. Am. Chem. Soc.* **2013**, *135*, 14871. (b) Nam, W.; Lim, M. H.; Oh, S.-Y.; Lee, J. H.; Lee, H. J.; Woo, S. K.; Kim, C.; Shin, W. *Angew. Chem., Int. Ed.* **2000**, *39*, 3646. (c) Nam, W.; Lee, H. J.; Oh, S.-Y.; Kim, J.; Jang, H. G. *J. Inorg. Biochem.* **2000**, *80*, 219.

(18) Arasasingham, R. D.; He, G.-X.; Bruice, T. C. *J. Am. Chem. Soc.* **1993**, *115*, 7985.

(19) Garrison, J. M.; Ostović, D.; Bruice, T. C. *J. Am. Chem. Soc.* **1989**, *111*, 4960.

(20) (a) Meunier, B.; Guilmet, E.; De Carvalho, M.-E.; Poilblanc, R. *J. Am. Chem. Soc.* **1984**, *106*, 6668. (b) Shaik, S.; Hirao, H.; Kumar, D. *Acc. Chem. Res.* **2007**, *40*, 532. (c) Kumar, D.; Karamzadeh, B.; Sastry, G. N.; de Visser, S. P. *J. Am. Chem. Soc.* **2010**, *132*, 7656.

(21) (a) Barone, V.; Cossi, M. *J. Phys. Chem. A* **1998**, *102*, 1995. (b) Cossi, M.; Rega, N.; Scalmani, G.; Barone, V. *J. Comput. Chem.* **2003**, *24*, 669.

(22) (a) Schubert, W. M.; Keeffe, J. R. *J. Am. Chem. Soc.* **1972**, *94*, 559. (b) Yates, K.; MacDonald, R. S.; Shapiro, S. A. *J. Org. Chem.* **1973**, *38*, 2460.

(23) (a) Cho, K.-B.; Shaik, S.; Naam, W. *J. Phys. Chem. Lett.* **2012**, *3*, 2851. (b) Kwon, E.; Cho, K.-B.; Hong, S.; Naam, W. *Chem. Commun.* **2014**, *50*, 5572.

(24) Jean, Y. *Molecular Orbitals of Transition Metal Complexes*; Oxford University Press Inc.: New York, 2005; p 61.